Weierstraß–Institut
für Angewandte Analysis und Stochastik

im Forschungsverbund Berlin e.V.

Preprint ISSN 0946 – 8633

Reflections of Eulerian shock waves at moving adiabatic boundaries

Wolfgang Dreyer, Matthias Kunik

submitted: 8th March 2000

Weierstrass Institute
for Applied Analysis and Stochastics
Mohrenstrasse 39
D – 10117 Berlin
Germany
E-Mail: dreyer@wias-berlin.de
E-Mail: kunik@wias-berlin.de

Preprint No. 383
Berlin 2000

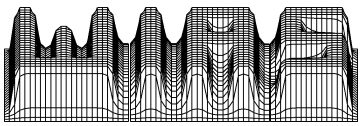

Edited by
Weierstraß–Institut für Angewandte Analysis und Stochastik (WIAS)
Mohrenstraße 39
D — 10117 Berlin
Germany

Fax: + 49 30 2044975
E-Mail (X.400): c=de;a=d400-gw;p=WIAS-BERLIN;s=preprint
E-Mail (Internet): preprint@wias-berlin.de
World Wide Web: http://www.wias-berlin.de/

Abstract

This study solves the initial and boundary value problem for the EULER equations of gases. The boundaries are allowed to move and are assumed to be adiabatic. In addition we shall discuss that isothermal walls are not possible within the EULER theory.

We do not formulate the boundary conditions in terms of the macroscopic basic variables mass density, velocity and temperature. Instead we consider the underlying kinetic picture which exhibits the interaction of the gas atoms with the boundaries. Hereby the advantage is offered to formulate the boundary conditions in a very suggestive manner.

This procedure becomes possible, because we approach the solution of the EULER equations by the following limit: We rely on the moment representation of the macroscopic basic variables, and in order to obtain the temporal development of the phase density, we decompose a given macroscopic time interval into periods of free flight of the gas atoms. These periods of duration τ_{ME} are interrupted by a maximization of entropy, thus introducing a simulation of the interatomic interaction. In [2] we have shown that the EULER equations may be established in the limit $\tau_{ME} \to 0$.

1 Introduction

For the most time, the atoms of a gas fly independent of each other through the volume at their disposal. From time to time there is a binary interaction of duration τ_C . We are only interested for situations where the mean time of free flight τ_R, also called relaxation time, is much larger than τ_C.

A further important characteristic time is given by the combination $\tau_G \left(M_a + 1\right)^{-1}$, which gives the duration of equalization of spatial inhomogeneiities. τ_G is called gradient time and M_a is a mean MACH number.

When the condition $\tau_R \gg \tau_G \left(M_a + 1\right)^{-1}$ is met, the gas develops mainly by free flight of its atoms. In this case the description of the thermodynamic state requires many

variables. In the other extreme case $\tau_R \ll \tau_G \left(M_a + 1\right)^{-1}$ there is a fast relaxation so that the atomic velocities $\mathbf{c}$ are distributed according to the MAXWELLIAN

$$f_M(t, \mathbf{y}, \mathbf{c}) = \frac{1}{m} \frac{\rho(t, \mathbf{y})}{(2\pi \frac{k}{m} T(t, \mathbf{y}))^{3/2}} \exp(-\frac{(\mathbf{c} - \mathbf{v}(t, \mathbf{y}))^2}{2\frac{k}{m} T(t, \mathbf{y})}). \tag{1}$$

The thermodynamic state is here described with sufficent accuracy by only five variables, viz. mass density ρ, momentum density ρv and energy density ρe. v denotes the velocity and the energy density is related to the temperature T in a monatomic gas by $\rho e = \rho u + \frac{\rho}{2} v^2 = \rho \frac{3}{2} \frac{k}{m} T + \frac{\rho}{2} v^2$. k denotes BOLTZMANN's constant, and m is the atomic mass.

The development of these fields in space and time are determined by the EULER equations whose weak form read in one space dimension

$$\begin{aligned} &\oint_{\partial\Omega} \left(\rho dx - \rho v dt\right) = 0, \\ &\oint_{\partial\Omega} \left(\rho v dx - \left(\rho v^2 + p\right) dt\right) = 0, \\ &\oint_{\partial\Omega} \left(\left(\rho u + \tfrac{\rho}{2} v^2\right) dx - \left(\rho u + p + \tfrac{\rho}{2} v^2\right) v dt\right) = 0, \end{aligned} \tag{2}$$

Here Ω is a convex set in space time with piecewise smooth, positive oriented boundary $\partial\Omega$. The pressure p in a monatomic ideal gas is related to the internal energy density ρu by $p = \frac{2}{3} \rho u$.

In addition to (2) we have to impose the following entropy-inequality:

$$\oint_{\partial\Omega} \left(h dx - h v dt\right) \geq 0, \tag{3}$$

where the entropy density is given as $h = \frac{3}{2} \frac{k}{m} \rho \ln u \rho^{-\frac{3}{2}}$. Note that in regular points (t, x) the inequality (3) reduces to the additional conservation law

$$\frac{\partial h}{\partial t} + \frac{\partial (hv)}{\partial x} = 0,$$

which in this case is already a consequence of (2), since (3) is the convex extension of (2).

To achieve shorthand notation we put together the volume densities and the fluxes according to

$$u_A = \left(\rho, \rho v_i, \rho e\right), \qquad F_{Ak} = \left(\rho v_k, \rho v_i v_k + p\delta_{ik}, \rho \left(e + \frac{p}{\rho}\right) v_k\right), \tag{4}$$

for $A = 0, 1, 2, 3, 4$ and $i, k = 1, 2, 3$. The weak form of the EULER equations and of the entropy inequality thus read in compact three dimensional form

$$\oint_{\partial\Omega} \left(u_A, F_{Ak}\right) \, d\vec{o} \; = \; 0, \qquad \oint_{\partial\Omega} \left(h, h v_k\right) \, d\vec{o} \geq \; 0, \tag{5}$$

where $d\vec{o}$ is a hypersurface element in space and time.

In [2] we have established a representation theorem that gives the unique global solution of the initial value problem of the EULER equations. Arbitrary, but bounded, initial data are allowed and all possible shock interactions are included.

The representation theorem relies on a modified *Maximum Entropy Principle* (MEP) and on the explicit knowledge on the free flight periods of the atoms. In short:

We consider a time interval $0 < \tau \leq \tau_{ME}$ and represent for fixed t and τ_{ME} the volume densities u_A and fluxes F_{Ak} by

$$\begin{aligned} u_A(t+\tau, \mathbf{x}) &= m \int_{-\infty}^{+\infty} c_A w_M \left(u_B\left(t, x-\tau\mathbf{c}\right), \mathbf{c}\right)\ d^3\mathbf{c}, \\ F_{Ak}(t+\tau, \mathbf{x}) &= m \int_{-\infty}^{+\infty} c_A c_k w_M \left(u_B\left(t, x-\tau\mathbf{c}\right), \mathbf{c}\right)\ d^3\mathbf{c}, \end{aligned} \tag{6}$$

as well as the entropy density h and entropy flux Φ_k by

$$\begin{aligned} h(t+\tau, \mathbf{x}) &= -k \int_{-\infty}^{+\infty} \left(w_M \ln \frac{w_M}{y}\right) \left(u_B\left(t, x-\tau\mathbf{c}\right), \mathbf{c}\right)\ d^3\mathbf{c}, \\ \Phi_k(t+\tau, \mathbf{x}) &= -k \int_{-\infty}^{+\infty} c_k \left(w_M \ln \frac{w_M}{y}\right) \left(u_B\left(t, x-\tau\mathbf{c}\right), \mathbf{c}\right)\ d^3\mathbf{c}, \end{aligned} \tag{7}$$

where $y = \left(\frac{m}{h_p}\right)^3$ and h_p is PLANCK's constant. Here c_A stands for $1, c_i, \frac{1}{2}c^2$. In this context $w_M(u_B(t,\mathbf{y}),\mathbf{c}) \equiv f_M(t,\mathbf{y},\mathbf{c})$ is just the Maxwellian phase density, written as a function of the fields u_B and of the microscopic velocity $\mathbf{c}$. Both notations of the Maxwellian are useful for different purposes.

At time $\tau = 0$, the Maxwellian w_M is *the* phase density that maximizes the entropy under prescribed $u_A(t,\mathbf{x})$. For $0 < \tau \leq \tau_{ME}$, w_M describes the free flight of the atoms, and at time $t+\tau_{ME}$ the entropy is again maximized, however, now under the constraints of fixed $u_A(t+\tau_{ME},\mathbf{x})$.

The weak form of the Euler equations and the entropy inequality follow in the limit $\tau_{ME} \longrightarrow 0$, which could be proved in [2] under the assumption of convergence. In addition, in [2] we have also proved (5) for $\tau_{ME} > 0$ with the quantities u_A, F_{Ak}, h and Φ_k given in (6) and (7).

This work grew out of the task to improve those parts of *Extended Thermodynamics* (ET) that regards the application to very low particle density and/or high MACH numbers. In ET these cases require the introduction of many moments of the phase density as thermodynamic variables. Alternatively, as we discussed in [2], very low particle density and/or high MACH numbers can be dealt thermodynamically with only few moments, if the free flight period of the atoms is explicitely taken into account by considering an appropriate value $\tau_{ME} > 0$. This is studied in [3]. In the current investigation we show

that the case $\tau_{ME} > 0$ is also best suited and presumably neccessary in order to be able to solve boundary value problems.

The modern *kinetic schemes* bear a strong resemblance to the current study. These were introduced independently of *ET* by B.PERTAME in [4], [5], [6] mainly for the Euler system and, relying on *ET,* by C.D. LEVERMORE [9] and by P. LE TALLEC & J.P. PERLAT [11] for higher order moment systems. Up to now the *kinetic schemes* as well as *ET* only consider the case $\tau_{ME} \to 0$. *ET* was brought into its present form by I. MÜLLER & I SHI LIU [7], [8].

The most important link between the purely macroscopic *ET* and the microscopic *kinetic theory* is the *Maximum Entropy Principle* (*MEP*). W. DREYER has shown for the first time in 1987 [1] that the *MEP* implies the phenomenological entropy principle of *ET*. A generalization of DREYER's reasonings was given in 1996 by G. BOILLAT & T. RUGGERI [10].

Now we proceed to extend the representation theorem to the complete initial *and* boundary value problem.

2 The Initial and Boundary Value Problem

In this section we shall discuss some peculiar features of the boundary value problem that shows the superiority of the microscopic based representation theorem (6) against the macroscopic point of view.

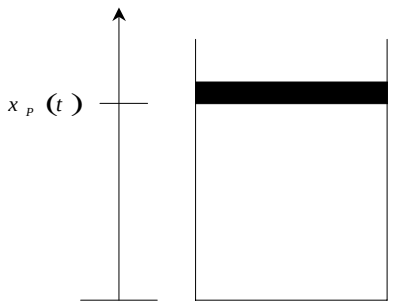

Fig. 1: Cylinder/Piston System

In order to be concrete we consider a one dimensional cylinder/moving piston system which is filled with a gas. The objective is the determination of the fields of density $\rho(t,x)$, velocity $v(t,x)$ and temperature $T(t,x)$. We assume that their initial data

$$\rho(0,x) = \rho_0(x)\,,\ v(0,x) = v_0(x)\,,\ T(0,x) = T_0(x) \tag{8}$$

are given, and we ask for possible boundary values at $x = 0$ and $x = x_P(t)$ so that a unique solution may exist.

We start the discussion from a macroscopic point of view. Obviously we should prescribe

$$v(t,0) = 0, \qquad v(t,x_P(t)) = \dot{x}_P(t)\,. \tag{9}$$

A study of the linear EULER problem reveals that this is already sufficient. However, properly one should think that it must be allowed to prescribe in addition to (9) the thermal properties of the walls under consideration. The condition (9) relies on the assumption of rigid walls and it seems natural to assign to the walls additionally either the property to be isothermal or to be adiabatic. In case of isothermal walls these must allow an energy flux in order to guarantee a prescribed temperature. In the adiabatic case the energy flux through the wall is zero with respect to an observer who moves with the wall. However, the isothermal wall is not possible here because (9) implies that the energy flux is already forced to zero.
To confirm in detail that isothermal walls are not possible within EULERs theory we consider an isothermal impermeable wall at rest, again in the one dimensional case.
It is due to the continuity equation $(2)_1$ that the macroscopic velocity is zero at the wall. On the other hand this implies due to the energy equation $(2)_3$ a vanishing energy flux at the wall. Note that within EULERs theory there is no non convective part of the energy flux. If there would be a non convective part then a vanishing velocity at the wall would not imply a vanishing heat flux. This can be realized in the case $\tau_{ME} > 0$.

3 A Reminder to the Numerical Scheme for the Initial Value Problem of the Euler System

In this section we give a short review of the numerical scheme presented in [2], where we solved the initial value problem for the weak EULER system in three space dimensions. In the next section, this scheme will be extended in order to include boundary conditions.

To initialize the scheme we start with:

- Bounded and integrable initial data for $\mathbf{x} \in I\!R^3$:
  $\rho(0,\mathbf{x}) = \rho_0(\mathbf{x}) \geq \epsilon > 0, \quad \mathbf{v}(0,\mathbf{x}) = \mathbf{v}_0(\mathbf{x}), \quad T(0,\mathbf{x}) = T_0(\mathbf{x}) \geq \delta > 0.$
- A fixed time $\tau_{ME} > 0$ of free flight, so that at the equidistant times $t_n = n\tau_{ME}$, $n = 0, 1, 2, ...$, the maximization of entropy takes place.

Within the time interval $0 < \tau \leq \tau_{ME}$ the iterated scheme for the variables density ρ,

velocity v and temperature T reads

$$\begin{aligned}
\rho(t_n+\tau,\mathbf{x}) &= \int_{-\infty}^{\infty} f_n(\mathbf{x}-\tau\mathbf{c},\mathbf{c})\; d^3\mathbf{c}, \\
(\rho v_i)(t_n+\tau,\mathbf{x}) &= \int_{-\infty}^{\infty} c_i f_n(\mathbf{x}-\tau\mathbf{c},\mathbf{c})\; d^3\mathbf{c}, \\
(\frac{1}{2}\rho\mathbf{v}^2+\frac{3}{2}\rho T)(t_n+\tau,\mathbf{x}) &= \int_{-\infty}^{\infty} \frac{1}{2}\mathbf{c}^2 f_n(\mathbf{x}-\tau\mathbf{c},\mathbf{c})\; d^3\mathbf{c}\ .
\end{aligned} \tag{10}$$

Here f_n is the three-dimensional MAXWELLIAN phase density, which we write now for the purposes of the numerical scheme :

$$f_n(\mathbf{y},\mathbf{c}) = \frac{\rho(t_n,\mathbf{y})}{(2\pi T(t_n,\mathbf{y}))^{3/2}} \cdot \exp(-\frac{(\mathbf{c}-\mathbf{v}(t_n,\mathbf{y}))^2}{2T(t_n,\mathbf{y})}). \tag{11}$$

All quantities of interest can again be brought into generic form. For $A = 0,...,4$; $k = 1,2,3$; $n = 0,1,2,...$ and $0 < \tau \leq \tau_{ME}$ we write for the variables u_A and fluxes F_{Ak}

$$\begin{aligned}
u_A(t_n+\tau,\mathbf{x}) &= \int_{-\infty}^{\infty} c_A f_n(\mathbf{x}-\tau\mathbf{c},\mathbf{c})\; d^3\mathbf{c}, \\
F_{Ak}(t_n+\tau,\mathbf{x}) &= \int_{-\infty}^{\infty} c_A c_k f_n(\mathbf{x}-\tau\mathbf{c},\mathbf{c})\; d^3\mathbf{c}\ ,
\end{aligned} \tag{12}$$

and for the entropy density h and entropy flux Φ_k

$$\begin{aligned}
h(t_n+\tau,\mathbf{x}) &= -\int_{-\infty}^{\infty} (f_n ln f_n)(\mathbf{x}-\tau\mathbf{c},\mathbf{c})\; d^3\mathbf{c}, \\
\Phi_k(t_n+\tau,\mathbf{x}) &= -\int_{-\infty}^{\infty} c_k (f_n ln f_n)(\mathbf{x}-\tau\mathbf{c},\mathbf{c})\; d^3\mathbf{c}\ .
\end{aligned} \tag{13}$$

Remarks:

- Note, that by definition of $c_A = \left(1, c_i, \frac{1}{2}c^2\right)$ the values u_A in (12) exactly agree with the moments given in (10), namely

$$u_0 = \rho,\ u_i = \rho v_i\ (i=1,2,3),\ u_4 = \frac{1}{2}\rho\mathbf{v}^2 + \frac{3}{2}\rho T. \tag{14}$$

- There are only two differences between the representations (12), (13) and (6), (7) : The equations above are written with the notation $f_n(\mathbf{y},\mathbf{c}) = w_M(u_B(t_n,\mathbf{y}),\mathbf{c})$, and the constants m, k, y are set equal to 1.

In [2] we have confirmed that this iterative scheme conserves mass, momentum and energy, and implies in addition the entropy inequality:

$$\oint_{\partial\Omega} (u_A\ , F_{Ak})\ \vec{do} = 0\ , \qquad \oint_{\partial\Omega} (\ h\ , \Phi_k\ )\ \vec{do} \geq 0\ , \tag{15}$$

even in the case $\tau_{ME} > 0$, as well as in the EULERian limit. Note that Ω is a set in space and time with positive orientated boundary $\partial\Omega$.
In the Eulerian limit, which is established for $\tau_{ME} \to 0$, the fields u_A, F_{Ak}, h and Φ_k just reduce to functions depending only on ρ, $\mathbf{v}$ and T. These will be given explicitely in the following section.

4 Boundary Conditions at Adiabatic and Moving Walls

In this section we generalize the numerical scheme from above to include boundary conditions. Our reasonings rely on the interaction of the gas atoms with the walls of the cylinder from Figure 1. The walls are assumed to be adiabatic, and because the piston is allowed to move, we have to describe the reflection of the atoms at adiabatic and moving walls.

Recall that in case of the pure initial value problem we prescribe the Maxwellian phase density at discrete maximization times t_0, t_1, t_2,.... In between two subsequent maximization times the phase density develops according to the free flight of the atoms. The period of free flight is now used to incorporate the boundary conditions.

In the following we restrict ourselves to one space dimension, but later it will become clear how to generalize the procedure to two or three space dimensions.

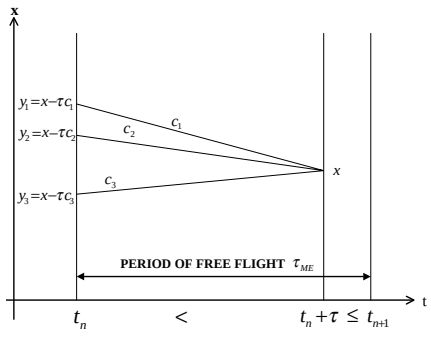

Fig. 2: Trajectories of free flight

The Figure 2 illustrates the procedure that we used for the initial value problem: Let x denote a position, where we want to compute the fields at time $t_n + \tau$. To achieve this goal we must know the fields at time t_n and at all positions $y_1 = x - \tau c_1$, $y_2 = x - \tau c_2$, $y_3 = x - \tau c_3$, ... which are formed with those microscopic velocities c that constitute the integration knodes. Geometrically speaking, we consider for given $x, t_n + \tau$ and c the free flight trajectory that links the point $t_n + \tau$, x with the point t_n , $y = x - \tau c$.

We shall observe now, that in case of boundaries, the trajectories that links $t_n + \tau$, x with t_n and some yet unknown position y^* turn out to be polygons instead of straight lines, because they may meet the walls several times within a period of free flight.

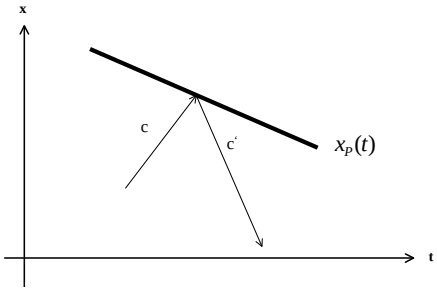

Fig. 3: Adiabatic Reflection

For the algorithmic procedure we assume that there is a piston located at position $x_P(t)$ at time t, where $0 \le t \le T$ and $x_P(t) \ge \epsilon > 0$ is a polygon. Let $v_P(t) = \dot{x}_p(t)$ be the velocity of the piston. If a particle with incoming velocity c is reflected at the piston at time t, it has an outgoing velocity $c^{'}$ according to

$$c + c^{'} = 2v_P(t). \tag{16}$$

This equation describes the elastic interaction of an adiabatic wall having infinite mass with a light particle. Furthermore we require an adibatic bottom at $x = 0$. Thus we have a one-

dimensional vessel with the piston as the upper boundary and the bottom as the lower one.

The adiabatic wall at the bottom $x = 0$ is at rest, which implies $c' = -c$. Of course this is a special case of (16).

The Figure 4 shows how to find the polygon that links $t_n + \tau$, x to t_n,y^* , where y^* is the corresponding position of the polygonal trajectory at time t_n. Recall that this was an easy task for the pure initial value problem, see Figure 2. As in Figure 2 we start here with given x and $t_n + \tau$ and any c. The trajectory $x - c\tau$ may now meet one of the walls and suffer a reflection. This may happen several times until the maximization time t_n is reached. The microscopic velocity which corresponds to this last part of the complete trajectory is denoted by c^*.

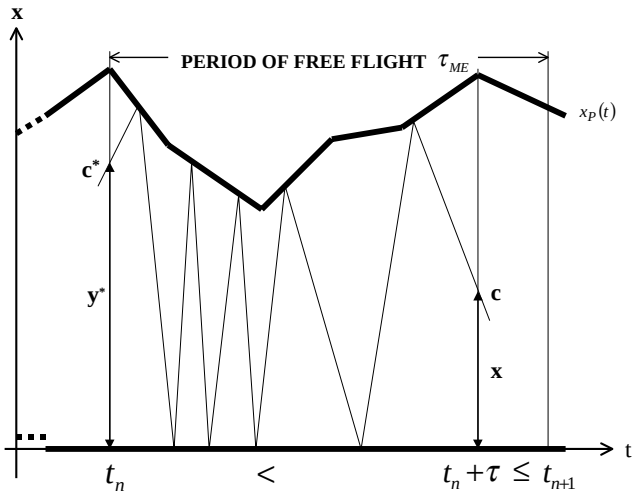

Fig. 4: The iterated functions y^* and c^*

Remarks:

- For a computation of the fields u_A at the intermediate time $t_n + \tau$ and the position x we need to know y^* and c^* which turn out to be functions of t_n, τ, x, c :
  $y^* = y^*(t_n, \tau, x, c)$ and $c^* = c^*(t_n, \tau, x, c)$. These functions have to be computed by an iterative procedure according to the reasonings that were given above.
- If there is no reflection for choosen values t_n, τ, x and c, then the functions y^* and c^* obviously reduce to $y^* = y = x - \tau c$ and $c^* = c$. These simple expressions are those we had already used for the pure initial value problem.

We make essential use of the functions y^* and c^* in the following scheme:

First we present the assumptions that are needed to formulate the numerical scheme for the initial and boundary value problem (in one space dimension):

- Bounded and integrable initial data for $x \in I\!R$:
  $\rho(0,x) = \rho_0(x) \geq \epsilon > 0, \quad v(0,x) = v_0(x), \quad T(0,x) = T_0(x) \geq \delta > 0.$
- For a free flight time $\tau_{ME} > 0$ fixed and equidistant times
  $0 = t_0 < t_1 < ... < t_N$, where $t_N = T > 0$, $t_i - t_{i-1} = \tau_{ME}$ and $i = 1, ..., N$.
- For $0 \leq t \leq T$ a polygon $x_P(t) > 0$.

Under these assumptions we may now state the representation of the solution of the initial and boundary value problem:

For $0 < \tau \leq \tau_{ME}$, $n = 0, 1, ..., N-1$, $0 \leq x \leq x_P(t)$ and $0 \leq t \leq T$ the solution reads

$$\begin{aligned} \rho(t_n + \tau, x) &= \int_{-\infty}^{\infty} f_n^{(1D)}(y^*, c^*)\ dc, \\ (\rho v)(t_n + \tau, x) &= \int_{-\infty}^{\infty} c f_n^{(1D)}(y^*, c^*)\ dc, \\ (\frac{1}{2}\rho v^2 + \frac{3}{2}\rho T)(t_n + \tau, x) &= \int_{-\infty}^{\infty} [\frac{1}{2}c^2 + T(t_n, y^*)] f_n^{(1D)}(y^*, c^*)\ dc\ . \end{aligned} \tag{17}$$

Here $f_n^{(1D)}$ is the **one-dimensional** Maxwellian phase density:

$$f_n^{(1D)}(y^*, c^*) = \frac{\rho(t_n, y^*)}{\sqrt{2\pi T(t_n, y^*)}} \cdot \exp(-\frac{(c^* - v(t_n, y^*))^2}{2T(t_n, y^*)}). \tag{18}$$

Before we shall discuss and motivate these representations, we continue with two

Remarks:

- In the scheme (17) the quantities which are indexed by "*" do only occur in the phase density $f_n^{(1D)}$ and in the temperature field T under the integral. The reason for this relies on the observation that those quantities have to be evaluated at the previous maximization time t_n, see Figure 4 for details.
- Since $x_P(t)$ is a polygon, which consists of finitely many straight lines, it can be shown by an induction conclusion that in general c^* is a discontinuous function of c with a finite number of jumps (for fixed t_n, τ and x) . These jumps result from the reflections of the trajectories at the adiabatic walls. In contrast, the function y^* is continuous everywhere. For this reasons the integrals (17) are well defined.

Now we extend the scheme (17) to the three dimensional case. The formulas that correspond to (17) will turn out to be more transparent. Vice versa the scheme in one space dimension results from the integration over the whole three-dimensional space of microscopic velocities.

To achieve the three dimensional scheme we first extend the initial data to three space dimensions. We define for $\mathbf{x} \in \{(x_1, x_2, x_3) \in I\!R^3 | 0 \leq x_1 \leq x_P(t)\}$ and the initial data given in one space dimension:

$$\begin{aligned} u_0(0, \mathbf{x}) &= \rho_0(x_1), \\ u_1(0, \mathbf{x}) &= \rho_0 v_0(x_1), \\ u_{2/3}(0, \mathbf{x}) &= 0, \\ u_4(0, \mathbf{x}) &= (\tfrac{1}{2}\rho_0 v_0^2 + \tfrac{3}{2}\rho_0 T_0)(x_1)\ . \end{aligned} \tag{19}$$

Next we extend the functions y^* and c^* as:

$$\begin{array}{rcl} \mathbf{y}^*(t_n,\tau,\mathbf{x},\mathbf{c}) & = & (y^*(t_n,\tau,x_1,c_1), \quad x_2-\tau c_2 \quad , \quad x_3-\tau c_3 \quad) \ , \\ \mathbf{c}^*(t_n,\tau,\mathbf{x},\mathbf{c}) & = & (c^*(t_n,\tau,x_1,c_1), \qquad c_2 \qquad , \qquad c_3 \qquad) \ . \end{array} \tag{20}$$

Hereafter we are able to introduce the fields and fluxes in its three-dimensional form according to

$$\begin{aligned} u_A(t_n+\tau,\mathbf{x}) &= \int_{-\infty}^{\infty} c_A f_n(\mathbf{y}^*,\mathbf{c}^*)\ d^3\mathbf{c} \\ F_{Ak}(t_n+\tau,\mathbf{x}) &= \int_{-\infty}^{\infty} c_A c_k f_n(\mathbf{y}^*,\mathbf{c}^*)\ d^3\mathbf{c}\ . \end{aligned} \tag{21}$$

We remind to the definition of the three-dimensional Maxwellian $f_n(\cdot,\cdot)$ given in (11) and conclude that u_A and F_{Ak} are independent on x_2 and x_3. After integration over c_2 and c_3, we obtain:

$$\begin{aligned} \rho(t_n+\tau,x_1) &= u_0(t_n+\tau,x_1,0,0), \\ (\rho v)(t_n+\tau,x_1) &= u_1(t_n+\tau,x_1,0,0), \\ (\frac{1}{2}\rho v^2+\frac{3}{2}\rho T)(t_n+\tau,x_1) &= u_4(t_n+\tau,x_1,0,0)\ , \end{aligned} \tag{22}$$

where $\rho(t_n+\tau,x_1)$, $(\rho v)(t_n+\tau,x_1)$ and $(\frac{1}{2}\rho v^2+\frac{3}{2}\rho T)(t_n+\tau,x_1)$ are given by (17).

Thus even in one space dimension the macroscopic fields (17) follow from the microscopically three-dimensional scheme (21).

Next we describe the behaviour of the macroscopic adiabatic boundary condition in the EULERian limit $\tau_{ME} \longrightarrow 0$. First of all we state that in the EULERian limit the dependence of (21) on $\mathbf{y}^*$ and $\mathbf{c}^*$ reduce to the simple expressions $\mathbf{y}^* = \mathbf{y} = \mathbf{x} - \tau\mathbf{c}$, $\mathbf{c}^* = \mathbf{c}$ that we have already obtained for the pure initial value problem. This is a consequence of the rapid decay of the MAXWELLian phase density regarding the $\mathbf{c}$ dependence.

Thus we conclude that the conservation laws and the entropy inequality, viz.

$$\oint_{\partial\Omega} (u_A\ , F_{Ak})\ \vec{do} = 0\ , \qquad \oint_{\partial\Omega} (\ h\ , \Phi_k\ )\ \vec{do} \geq 0\ , \tag{23}$$

are still valid in the EULERian limit, where the dependence of u_A , F_{Ak} , h and Φ_k on ρ , v and T is the same as in the pure initial value problem, viz.

$$u_A = \begin{pmatrix} \rho \\ \rho v_i \\ \rho\frac{v^2}{2}+\frac{3}{2}\rho T \end{pmatrix}\ , \qquad F_{Ak} = \begin{pmatrix} \rho v_k \\ \rho v_i v_k + \rho T\delta_{ik} \\ \rho\left(\frac{v^2}{2}+\frac{5}{2}T\right)v_k \end{pmatrix}\ , \tag{24}$$

$$h = \frac{3}{2}\rho \ln\left(T\rho^{-\frac{2}{3}}\right)\ , \qquad \Phi_k = h v_k . \tag{25}$$

The only additional condition for the boundary value problem in the Eulerian limit is in one space dimension

$$v\,(t,0) = 0, \qquad v\,(t,x_P\,(t)) = \dot{x}_P\,(t)\,. \tag{26}$$

5 Appropriate Integration Limits c_{min}, c_{max}

For evaluation of the representations (17), the c-integration has to be carried out over the whole real axis. However, since the MAXWELLian phase density (18) decays rapidly to zero with respect to c, we only have to consider a finite c-interval, where the MAXWELLian density gives a relevant contribution. It is the purpose of this section to determine such an appropriate (one-dimensional) integration interval $[c_{min}, c_{max}]$.

We define at a fixed maximization time t_n:

$$\begin{aligned} v^*_{min} &= \min_{0 \le y^* \le x_P(t_n)} v(t_n, y^*), \\ v^*_{max} &= \max_{0 \le y^* \le x_P(t_n)} v(t_n, y^*), \\ T^*_{max} &= \max_{0 \le y^* \le x_P(t_n)} T(t_n, y^*). \end{aligned} \tag{27}$$

If we set for some positive constant γ

$$c^*_{min} = v^*_{min} - \gamma\sqrt{2T^*_{max}} \quad , \quad c^*_{max} = v^*_{max} + \gamma\sqrt{2T^*_{max}} \quad , \tag{28}$$

we obtain for the appropriate choice $\gamma = 4$ and for each c^* outside the interval $[c^*_{min}, c^*_{max}]$

$$e^{-\frac{(c^* - v(t_n, y^*))^2}{2T(t_n, y^*)}} < e^{-\gamma^2} = e^{-16} = 1.125...10^{-7} \ . \tag{29}$$

In order to guarantee the condition (29) we have to solve the following problem:

Seek for two limits c_{min}, c_{max} at time $t_n + \tau$ such that for all x with $0 \le x \le x_P(t_n + \tau)$ the "projection"-velocity $c^*(t_n, \tau, x, c)$ lies outside $[c^*_{min}, c^*_{max}]$ whenever c lies outside $[c_{min}, c_{max}]$. In addition, we require that these limits should be choosen as narrow as possible.

This problem will be solved by the following procedure: We decompose $[t_n, t_{n+1}]$ in F subintervals of the same length according to

$$t_{n,j} = t_n + j\frac{t_{n+1} - t_n}{F} \quad , \quad (j = 0, ..., F) \ . \tag{30}$$

Then $t_{n,0} = t_n$ and $t_{n,F} = t_{n+1}$. Now we assume that the polygon $x_P(t)$ is **linear** for each subinterval $[t_{n,j}, t_{n,j+1}]$, $(j = 0, ..., F-1)$, which is illustrated in the following sketch:

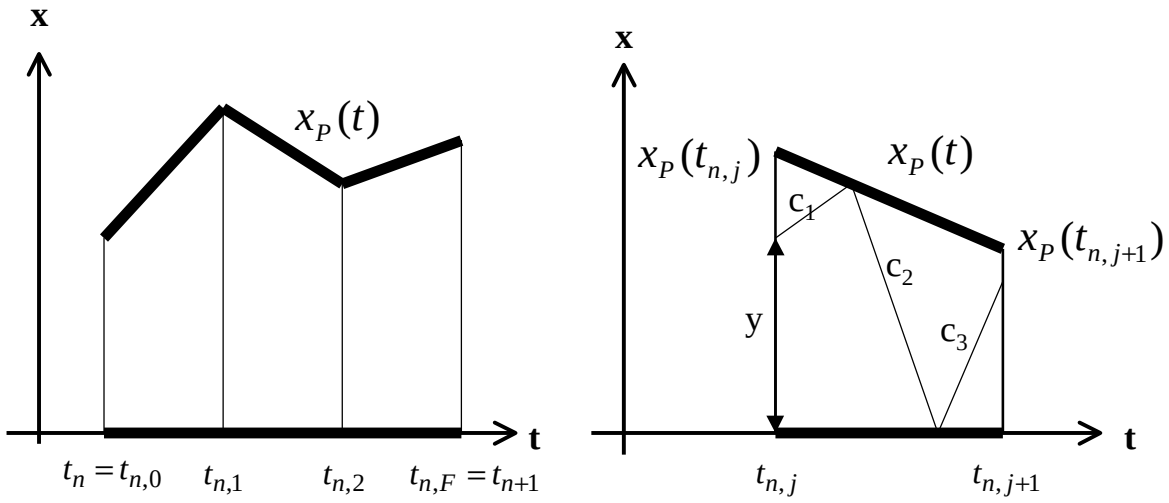

Fig. 5: Subdecomposition of the free flight interval $[t_n, t_{n+1}]$

From the right sketch above we may also read off definitions of two auxiliary functions

$$cmin_j(y, c_1) = min(c_1, c_2, c_3, ...) \ , \ cmax_j(y, c_1) = max(c_1, c_2, c_3, ...) \ . \tag{31}$$

These are defined for $0 \leq y \leq x_p(t_{n,j})$.

Now we are able to formulate the scheme for c_{min}, c_{max}:

- Initialization at time t_n: $c^0_{min} = c^*_{min}$, $c^0_{max} = c^*_{max}$.
- Iteration:

$$\begin{aligned} c^{j+1}_{min} \ = \ min[\ & cmin_j(\ 0 \ , c^j_{min}), \ cmin_j(\ 0 \ , c^j_{max}), \\ & cmin_j(\ x_p(t_{n,j}) \ , c^j_{min}), \ cmin_j(\ x_p(t_{n,j}) \ , c^j_{max}) \ ] \end{aligned} \tag{32}$$

$$\begin{aligned} c^{j+1}_{max} \ = \ max[\ & cmax_j(\ 0 \ , c^j_{min}), \ cmax_j(\ 0 \ , c^j_{max}), \\ & cmax_j(\ x_p(t_{n,j}) \ , c^j_{min}), \ cmax_j(\ x_p(t_{n,j}) \ , c^j_{max}) \ ] \end{aligned} \tag{33}$$

Then for $\tau = j\frac{t_{n+1}-t_n}{F}$, i.e. $t_n + \tau = t_{n,j}$, the values $c_{min} = c^j_{min}$ and $c_{max} = c^j_{max}$ have the desired properties.

Remark: Note that the time for computing c_{min} , c_{max} may be neglected, since this procedure is called only once at each new time step $t_{n,j}$: Hereafter we can use these values

for all integrations at each position x for that fixed time. In order to carry out the integrations, even the simple trapezium rule gives astonishing results. This is demonstrated in chapter 6.

If one prefers to use higher order integration methods, like Simpson's rule or the Gaussian integration method, one has to take care of the discontinuities of the function $c^*(t_n, \tau, x, c)$ which are caused by the adiabatic wall reflections.

6 Some Initial and Boundary Value Problems

For an illustration of the formalism we consider four initial boundary value problems in the sequel.

6.1 The Effect of Different Distances Between Entropy Maximizations

The first example may serve to illustrate the effect that a given time interval is decomposed into different numbers of maximization times t_n. We consider a one dimensional cylinder which is closed by two fixed adiabatic walls at $x = 0$ and $x = 2$. The cylinder contains a gas whose initial state at $t = 0$ is given by

$$\rho\,(0,x) = \begin{cases} 2 & , \quad x \leq 1 \\ 1 & , \quad x > 1\ , \end{cases} \qquad v\,(0,x) = 0, \qquad T\,(0,x) = 1. \tag{34}$$

At the boundaries the atoms are assumed to be reflected elastically so that it is guaranteed that there is no flux of mass and energy through the walls.

Figure 6 contains two columns which show the fields of density, velocity and temperature within the range $0 \leq t \leq 3$, $0 \leq x \leq 2$. The first column corresponds to 10 periods of free flight, while the second column is generated with 150 periods. The latter case almost establishes the EULERian limit.

Fig. 6: Effect of different periods of free flight

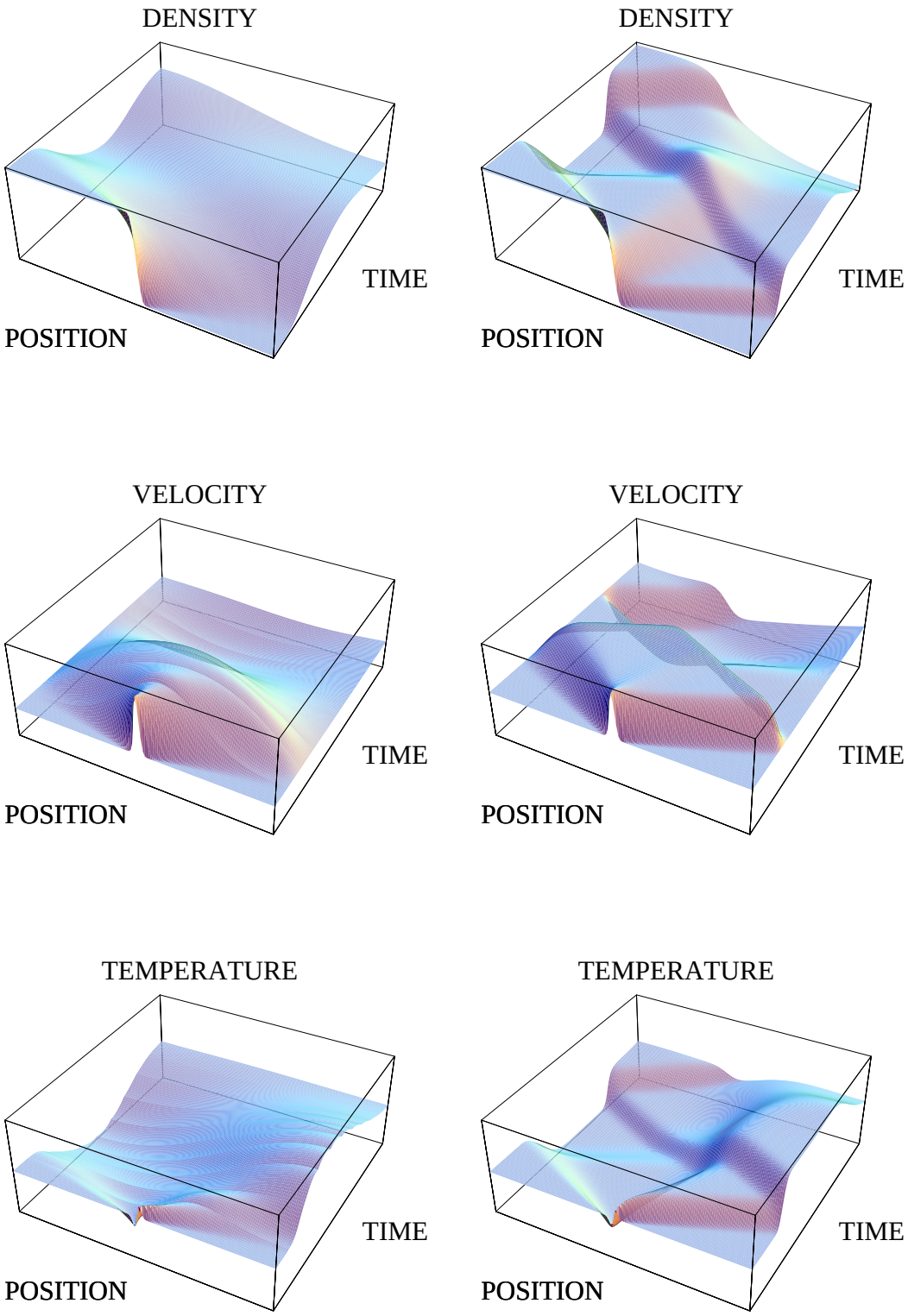

The first column exhibits the effect of the interruption of the free flight period by a maximization. Physically speaking, the maximization destroys the knowledge on the previous period. Thus particle interaction is introduced only implicitely here by maximization of entropy at discrete times whereas the gas develops according to the free flight of its atoms between the maximization times. However, one may wonder why interruption of the free flight period by the maximization process seems to appear only in the velocity and in the temperature field. All three fields are by construction of course continuous at the maximization times, but only the densitiy has also a continuous time derivative. The reason for this is, that the density is the only field whose flux is also a variable which thus appear due to the maximization process in the phase density. The fluxes of momentum and energy density do not occur among the variables and are thus discontinuous at the maximization times because these do not appear in the phase density. This implies the discontinuity of the time derivatives of velocity and temperature at the maximization times.

6.2 Propagation of an Initial Density Pulse Between Stationary Adiabatic Walls

The next example shows the production of entropy that accompanies the development of strong shocks. We consider again a one dimensional cylinder which is closed by two fixed adiabatic walls at $x = 0$ and $x = 4$. The cylinder contains a gas whose initial state at $t = 0$ is given by

$$\rho(0,x) = \begin{cases} 4 & , \quad 1.5 \leq x \leq 2.5 \\ 1 & , \quad otherwise \end{cases}, \qquad v(0,x) = 0, \qquad T(0,x) = 1. \tag{35}$$

Figure 7 shows contour plots of the fields of density, velocity and temperature and their temporal development. Both discontinuities of the initial density pulse split off into three disturbances which propagate with one of the three possible speeds that the Euler system offers. Furthermore, at its initial discontinuities the density pulse has created disturbances in the velocity and the temperature of the gas. All these disturbances interact with each other and give rise to a complex wave structure. The fastest disturbances move straight to the walls where they suffer a reflection. The reflected waves interact with the remaining unreflected waves which in turn lead in particular to a concentration in the middle of the cylinder at about $t \approx 1.8$. The extrem values are $\rho Min = 0.95$, $\rho Max = 4.00$, $vMin = -0.59$, $vMax = 0.59$, $TMin = 0.53$, $TMax = 1.66$.

Figure 7 also shows the temporal development of the entropy $H(t)$ and its density $h(t,x)$. Obviously $H(t)$ is an increasing function of time. Note that the entropy density $h(t,x)$ is almost a discontinuous function because we have decomposed the time interval $[0,3]$ into 400 periods of free flight corresponding to 400 maximizations. This represents almost the EULERian limit.

Fig. 7 Interaction of Shock Waves

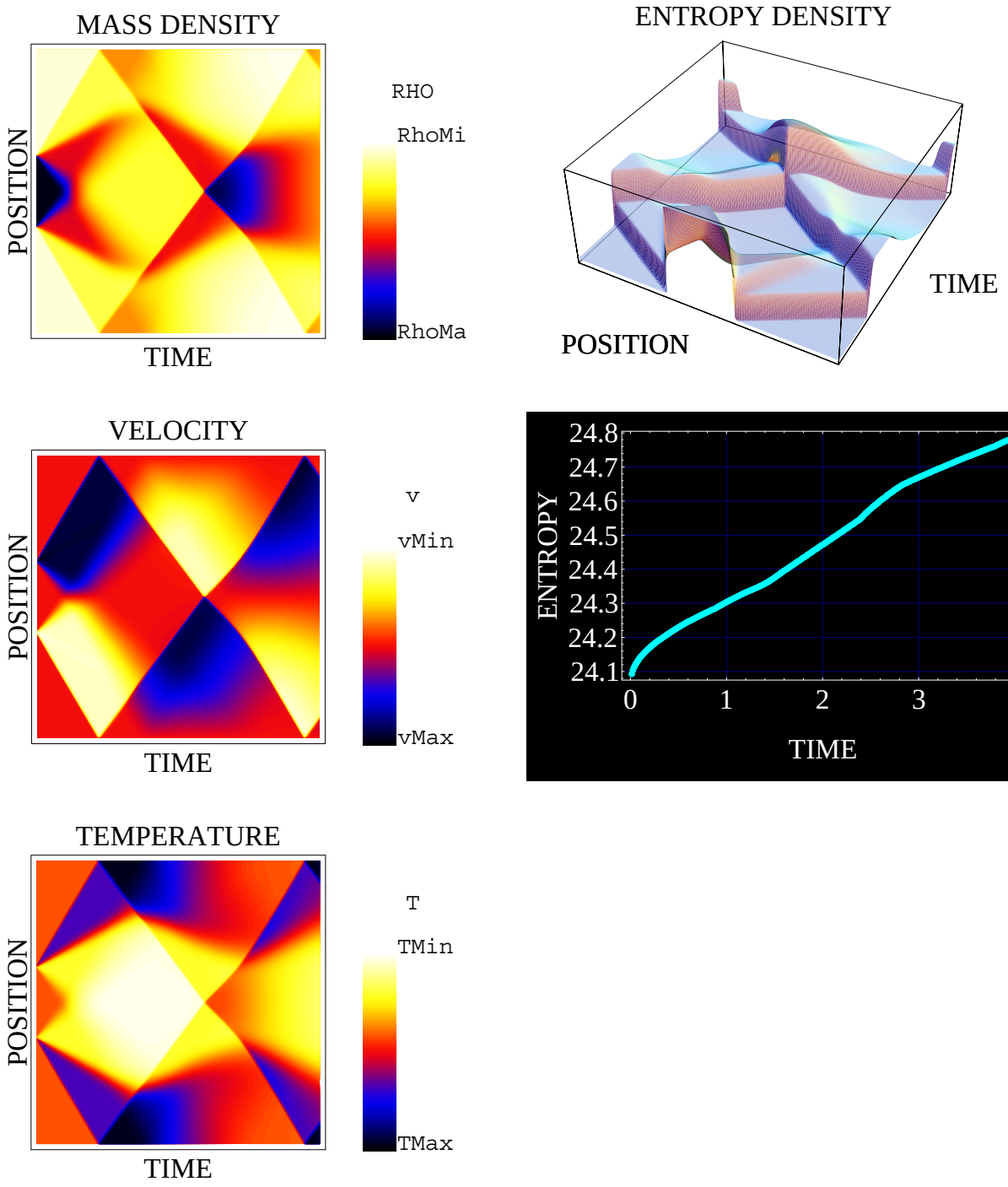

6.3 Creation of Shock Waves by a Moving Piston

At first we consider an adiabatic piston that moves into the cylinder according to the law $x_P(t) = 4(1 - 0.6\sin(t))$, where t is out of the range $[0, 3]$. The initial data are

$$\rho(0, x) = 1, \qquad v(0, x) = 0, \qquad T(0, x) = 1. \tag{36}$$

Since the speed of the piston is unequal to zero already at the beginning $t = 0$, a shock wave appears immediately and propagate into the homogeneous, undisturbed gas ahead of the piston. After some time the shock wave is reflected at the bottom and runs into the now disturbed gas up to the time where there is another reflection at the piston, and so on. The global solution is illustrated in the left column of Figure 8.

Next we consider an adiabatic piston that moves into the cylinder according to the law $x_P(t) = 3 - 0.5t^2$, starting at time $t = 0$. From time $t = 2.1$ on, the piston is stopped up to the final time $t = 4$. The initial data are again

$$\rho(0, x) = 1, \qquad v(0, x) = 0, \qquad T(0, x) = 1. \tag{37}$$

The resulting solution is depicted in the right column of Figure 8. In this case, the initial speed of the piston is zero, and for this reason the fields are continuous up to the critical $t_{crit} = \frac{3}{4}\sqrt{\frac{5}{3}} \approx 0.97$. However, because the initial acceleration of the piston is unequal to zero, a so called acceleration wave appears. The discontinuity of $\frac{\partial v}{\partial t}$ propagates with the speed of sound $\sqrt{\frac{5}{3}}$ into the undisturbed gas. It is due to HADAMARDs lemma that a discontinuity of one variable, here $\frac{\partial v}{\partial t}$, must be accompanied by discontinuities of all derivatives of all variables with respect to space and time.

Note that the expression $t_{crit} = \frac{3}{4}\sqrt{\frac{5}{3}}$ results from a long and cumbersome calculation of the development of weak discontinuities.

When the critical time is approached the discontinuities in the derivatives tend to infinity and thus give rise to the appearance of discontinuities of the variables themselves. A shock is created which still moves into the undisturbed region until the bottom is reached for the first time. There the first reflection of the shock wave takes place which forces the shock to move back to the piston, where the second reflection takes place, and so on.

Fig. 8 Shock Waves and Acceleration Waves

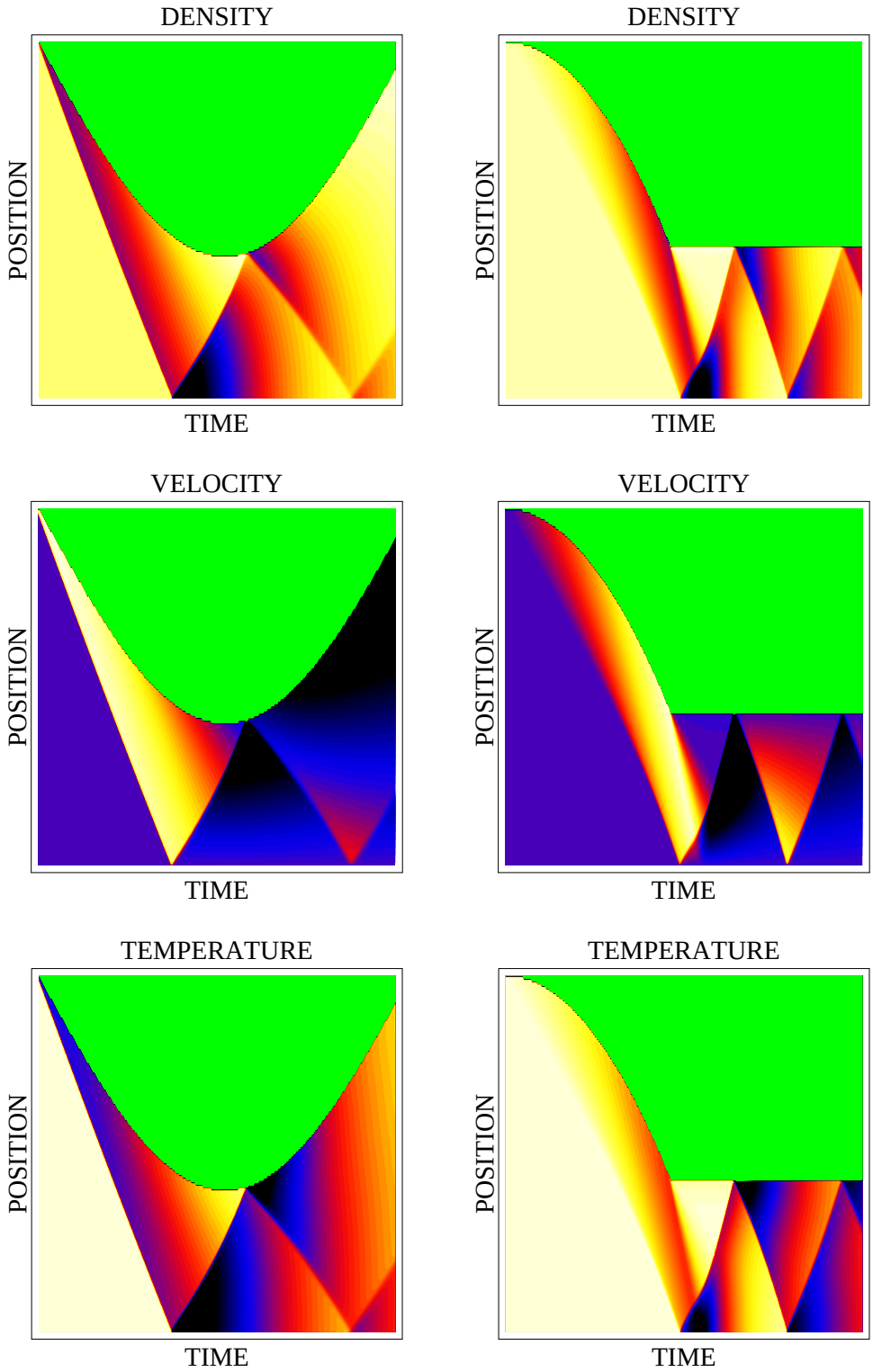

References

[1] W. Dreyer, *Maximization of the entropy in non-equilibrium*, J. Phys. A.: Math. Gen. 20 (1987).

[2] W. Dreyer, M. Kunik, *The maximum entropy principle revisited*, Preprint No. 367 (1997), WIAS Berlin. Submitted to Annales de l'Institute Henri Poincare

[3] W. Dreyer, M. Kunik, *Between Extended Thermodynamics with 10 Fields and Navier Stokes*, In preparation

[4] B. Pertame, *Boltzmann type schemes for gas dynamics and the entropy property*, SIAM J. Numer. Anal. 27 (6) (1990), pp 1405-1421.

[5] B. Pertame, *Second order Boltzmann schemes for compressible Euler equations in one and two space variables*, SIAM J. Numer. Anal. 29 (1) (1992), pp 1-19 .

[6] B. Pertame, *The kinetic approach to systems of conservation laws, recent advances in partial differential equations*, editors

M. A. Herrero and E. Zuazua, Wiley and Mason (1994), pp. 85-97.

[7] I. S. Liu, I. Müller,. *Extended Thermodynamics of classical and degenerate gases,* Arch. Rat. Mech. Anal. 83 (1983).

[8] I. Müller, *Thermodynamics.* Pitman Advanced Publishing Program, Boston (1985).

[9] C. D. Levermore, *Moment closure hierarchies for kinetic theories,* J. Stat. Phys. 83 (1996), pp. 1021-1065.

[10] G. Boillat, T. Ruggeri, *Moment equations in the kinetic theory of gases and wave velocities*, Pys. Rev. B. in press.

[11] P. L. Tallec, J. P. Perlat, *Numerical analysis of Levermore's moment system*, Preprint No. 3124, INRIA, Le Chesnay Cedex (France) (1997).